

## ST-008 Appendix IX. PROJECT TEST RESULTS

### Introduction

Ingios COMP-Score RT provides real-time monitoring of compaction measurements to aid in earthwork and pavement foundation compaction process and quality assessment. Compaction equipment is outfitted on any vibratory smooth drum roller (in less than 1 day) with state-of-the-art hardware for measuring, recording, and visually monitoring the results of the compaction process. Once outfitted, a field calibration process involving the Automated Plate Load Testing (APLT) system is implemented.

COMP-Score RT uses advanced data analytics and requires site specific calibration of the roller sensor measurements using in situ plate load test measurements (i.e., modulus of subgrade reaction, in situ elastic modulus, or in situ resilient modulus), and uses the full spectrum of the drum acceleration signature. This allows the monitoring equipment to deliver a high degree of reliability in the predicted measurements. Recent field calibrations on subgrade and base materials using this approach showed coefficient of determination ( $R^2$ ) > 0.9 are achievable using this technique (compared to  $R^2$  of 0.6 using compaction meter value (CMV) for the same data (White et al. 2014)). Another recent example was on a recent construction site on an Illinois Tollway construction project west of O'Hare airport (White et al. 2018, Tutumluer et al. 2018), which showed a  $R^2$  of 0.27 for predicting  $M_{r-Comp}$  using CMV versus  $R^2 = 0.93$  using the COMP-Score RT approach. Similarly, calibration using CMV for predicting static plate load test modulus of subgrade reaction ( $k$ ) value produced  $R^2$  of 0.74 versus  $R^2 = 0.96$  using the COMP-Score RT approach. White and Vennapusa (2017) recently documented calibration results with stress-dependent  $M_r$  values with  $R^2$  values  $\sim 0.9$  or greater, from testing on MnROAD field test sections in Albertville, MN with foundation layers consisting of granular and non-granular materials with varying stiffness and layered conditions.

The advantage with the COMP-Score RT approach is that the site calibration process significantly reduces the measurement error associated with the correlation, and the calibration relationships can be reliably used to develop the desired mechanical property maps.

During contractor production operations, the RT technology also uses advanced algorithms to provide real-time feedback of the compaction operations. COMP-Score RT also independently verifies to the project engineering team that the contractor's work: (1) achieves the minimum critical engineering parameter values (e.g., in-situ  $k$ -value) over a defined percentage (e.g., 80 to 90%) of the area monitored; (2) limits the variability of critical engineering parameter values of the area monitored; and (3) restricts the size of localized contiguous areas of non-compliance (i.e., "soft spot").

For this project, a CS56 smooth drum vibratory roller weighing approximately 27,450 lbs outfitted with Ingios RT retrofit system was used (Figure 1). Calibration was developed from APLT results to output stress-dependent  $k$  and  $M_r$  values (Figure 2).



**Figure 1 .Caterpillar CS56 vibratory smooth drum roller outfitted with Ingios COMP-Score RT system and GPS.**



**Figure 2. Automated Plate Load Testing trailer.**

## Definitions

### *COMP-Score® RT Technology*

Ingios COMP-Score® RT involves installing a computer/sensor(s) on a soil compaction machine and displaying sensor data to the operator whereby the operator then makes decisions on how best to use the compaction machine to meet compaction target values for the project. The data is presented real-time as color-coded geospatial maps. The compactor is outfitted with GPS equipment to measure drum location which is coordinated with data to create color-coded compaction maps.

### *Applications*

Contractors (local and remotely), Engineers (remotely), and Owners (remotely). Contractors use the real-time data at the operator and project superintendent levels. Engineers use the data to assess quality control and assurance requirements (with results generated within minutes). Owners use the data to validate and document construction, and longer-term, link mapping results to life-cycle cost analysis. The value of the RT data is time-dependent and different for different users. Users access the COMP-Score CONNECT web portal via desktop/laptop computer or mobile device.

### *Key Features and Scenarios*

The compaction machine on the project is setup with the Ingios COMP-Score RT system to collect and present data to the operator. The operator views geospatial and color-coded map results overlain on georeferenced aerial photo and then makes improved decisions about compaction process (e.g., number of roller passes require and other process control decisions such as moisture control). Non-operator users will access the real-time results via a remote desktop application and then receive e-Compaction reports via email/text. Ingios technology is state of-the-art both in terms of the hardware/quality of data and with customized analytics for the project.

### *Compliance*

Ingios data is calibrated with independent testing and validated whereby the data is compared to calibration limits that are preset in the machine. The data output is strictly controlled by Ingios and not the contractor (machine operated per Ingios requirements). Data results are reported as invalid if the compaction machine is not operated per the calibration requirements for compaction amplitude and vibration frequency.

### *Software Architecture*

The computer on the compaction machine runs Windows 7/10 and is connected to the internet via LTE mobile gateway. Data on the compaction machine is collected using Ingios proprietary software and security applications. The raw data exported from the

machine is collected, sent to a server (Microsoft Azure), filtered, analyzed, backed-up, and is then available for report generation.

### *Remote Real-Time Monitoring Services*

Users who want to view the data in real-time (via laptop and mobile devices), can view the data through COMP-Score CONNECT dashboard.

### *e-Compaction Report*

Once the operator is done “mapping” an area with the compaction machine, the operator pushes a button that triggers the raw data file to be submitted automatically into a folder on Ingios server. Ingios software tools read the data and automatically generate the e-Compaction report. The compaction report includes various data analytics/statistical summaries and various plots of color-coded information (see Appendix VIII). A “clean” data file including all data analytics and positional coordinates on a 1 ft x 1 ft grid using state plane coordinates is made available to the user.

### *Email/Text Alert*

When a e-Compaction report is initiated, completed, downloaded, and report generated, email alerts are automatically sent to users associated to the project.

### *Control Charts*

Using results from the individual e-Compaction reports, COMP-Score CONNECT dashboard provides a summary of values on a timeline plot to display selected statistical parameter values over time. The generated e-Compaction report is available for quick reference by clicking on any of the data points presented on the control charts.

### *Quality Indices*

**Percent Passing Target Values:** % passing the target values is based on the number of geospatial grid points from the output that meet or exceed the minimum target engineering parameter value (e.g., k-value) for the selected material.

**Compaction Quality Index (CQI):** Compaction quality index (CQI) is a relative compaction index based on the percentage of the geospatial area that meets the minimum target values for the set engineering parameter value that accounts for the uniformity of compaction using a weighting factor. The default minimum target CQI is 95% using a uniformity weight factor of 50%.

$$CQI = 100 - (Min.TV \% Passing - Measured \% Passing) - [(Measured COV - Max.TV \% COV) * Uniformity Weighting Factor]$$

Calibration Quality Check: Ingios calculates statistical parameters that can be used to assess the “spread” of the compaction data relative to the allowable spread of the data based on the lower and upper limits of a calibration data set. These indices are traditionally applied for assessing data within control limits in production work. Ingios uses calibration index value to assess variation and centralization between the upper and lower limits determined from in situ calibration testing. The calibration index (CI) parameter provides a measure of whether the calibrated measurements (i.e., predicted k-value) are within or out of calibration. CI parameter value is determined for each production map, using the calibration test results as follows:

$$CI = \min\left(\frac{UL - \mu}{3\sigma}, \frac{\mu - LL}{3\sigma}\right)$$

where,  $UL$  = upper limit of the calibration;  $LL$  = lower limit of the calibration;  $\mu$  = calculated average of the predicted value, and  $\sigma$  = calculated standard deviation of the predicted values.

- If  $CI < 0$  = reported values are outside calibration limits.
- If  $CI < 0.5$  = Some reported values are outside calibration limits.
- If  $0.5 > CI < 1.0$  = Most of the reported values are within calibration limits.
- IF  $CI > 1.0$  = All reported values are within calibration limits.

## Statistical Sampling for Calibration

A valid field calibration effort should require statistical determination of the minimum number of test measurements needed to achieve a desired level of reliability and confidence level in future predictions. The minimum sample size needed for this calibration effort was determined using a procedure recommended by Dupont and Plummer (1998). The inputs needed to determine the minimum sample size include the mean and coefficient of variation (COV) of the measured and the predicted values, standard error of the regression fit, the expected slope of the regression fit between the measured and the predicted values, and desired confidence level in the future estimates. These inputs are first estimated based on prior testing/experience and are later clarified based on the in situ calibration test results.

## Field Projects

To conduct field demonstrations in the State of Iowa, the project team worked with the Iowa DOT and the Contractor personnel on eleven DOT and two County projects during the 2019 and 2020 construction season. Figure 3 shows the project locations, where the technologies have been deployed, and Table 1 summarizes additional information regarding each of the projects.

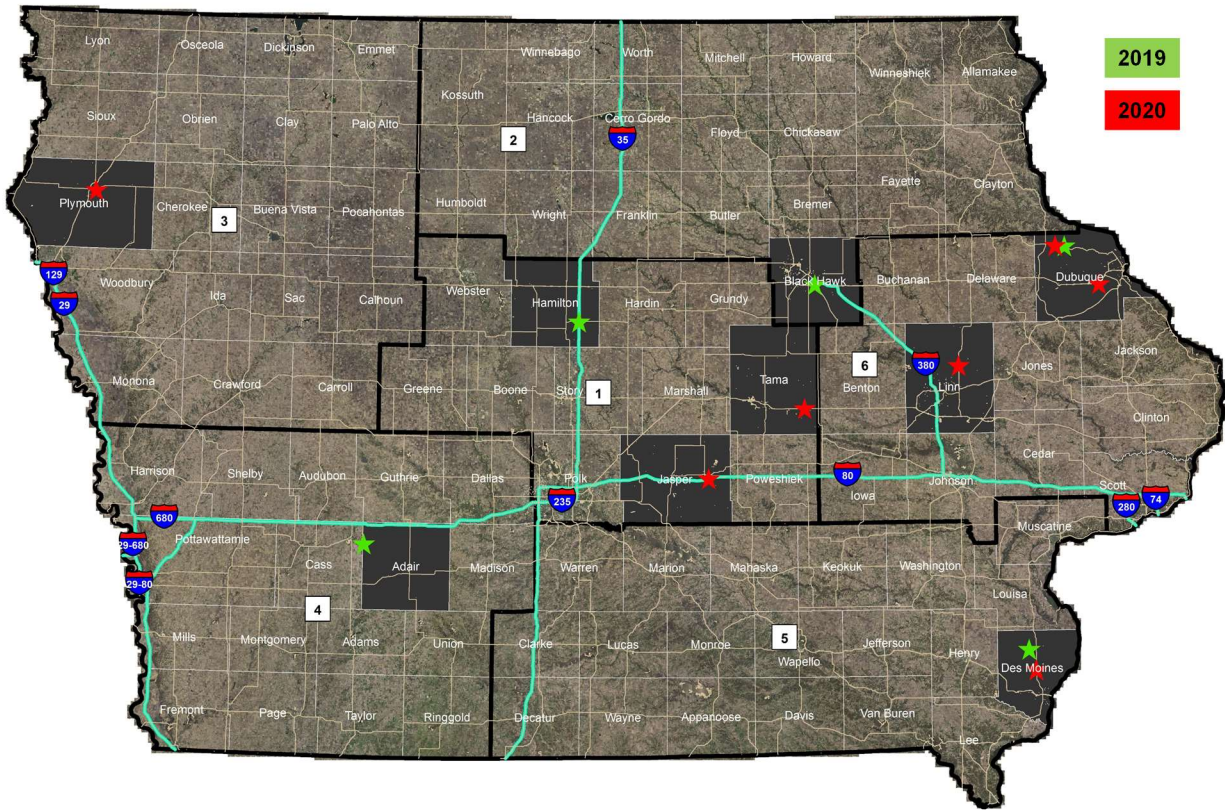


Figure 3. Project demonstration locations in 2019 and 2020.

Table 1. 2019 and 2020 Project Summary

County	Project Number	Contractor	Type of Project
<b>2019 Demonstration Projects</b>			
Blackhawk	NHSX-020-6(71)--3H-07	Cedar Valley	PCC Pavement
Hamilton	IM-035-5(111)133--13-40	CJ Moyna	PCC Pavement
Dubuque	HSIPX-052-2(120)--3L-31	CJ Moyna	PCC Pavement
Adair	LFM-LGG27--7X-01	County	Grading
Des Moines	L-P103GRADE--73-29	County	Grading
Des Moines	NHSX-061-2(62)--3H-29	Ames Construction	Grading
<b>2020 Demonstration Projects</b>			
Des Moines	NHSX-061-2(68)--3H-29	Streb Construction	PCC Pavement-New
Dubuque	NHSX-052-2(121)--3H-31	CJ Moyna & Sons	PCC Grade and Replace
Dubuque	NHSX-020-9(183)--3H-31	CJ Moyna & Sons	PCC Pavement-Grade and New
Jasper	IM-NHS-080-5(303)174--03-50	Peterson Contractors	PCC Pavement-Grade and New
Linn	NHSX-013-1(53)--3H-57	CJ Moyna & Sons	PCC Grade and Replace
Plymouth	NHSX-075-2(96)--3H-75	Peterson Contractors	PCC Grade and Replace
Tama	NHSX-030-6(191)--3H-86	Manatts	PCC Pavement-New

## Laboratory Characterization of Project Materials

A summary of laboratory index property test results for the materials tested as part of this project is provided in Table 2.

Additional lab testing results by the Michigan State University research group including laboratory permeability and resilient modulus testing (per AASHTO T307 loading sequence on prismatic samples) results at different compaction efforts are included in Appendix A. In the appendix, the results of sieve analyses and specific gravity, Atterberg limits, standard Proctor compaction, permeability, and laboratory resilient modulus (MR) tests are presented for the materials collected from 5 project sites [Dubuque County (US-52), Plymouth County (US-75), Linn County (US-13), Tama County (US-30), and Des Moines County (US-61)]. These materials were a mixture of reclaimed asphalt pavement (RAP) and reclaimed Portland cement concrete (RPCC) materials (modified subbase from US-52), a RAP material (special backfill from US-75), an RPCC material (granular subbase from US-13), crushed limestone aggregates (referred to as Crushed Limestones – granular subbases from US-30 and US-61), and subgrade (SG) materials (from US-30 and US-61).

Dry & wet sieve analyses and specific gravity and Atterberg limits tests were performed to classify these materials based on their index properties. Then, standard Proctor compaction tests were conducted to determine the optimum moisture content (OMC) and maximum dry unit weight (MDU) values of these materials. Based on standard Proctor compaction test results, a series of permeability and MR tests were performed.

Hydraulic conductivity tests were conducted on all materials at 95, 90, and 85% compaction levels to see the effect compaction on permeability (K). Test results showed that a decrease in the compaction level caused an increase in the K values. However, this reduction in drainage characteristics was not as significant and impactful compared to the reduction in stiffness values of the materials at lower compaction levels. Open graded materials (US-30 (CL) and US-61 (CL)) had the highest K values at each compaction level.

MR tests were performed on US-52 (RAP & RPCC), US-75 (RAP), US-13 (RPCC), US-30 (SG), and US-61 (SG) at 95, 90, and 85% compaction levels to see the effect of compaction on MR. Results are summarized in Table 3. Overall, test results showed that a decrease in the compaction level caused a decrease in the MR values (at the 6<sup>th</sup> loading sequence) and increase in plastic strain at the end of the test. While the MR values of US-52 (RAP & RPCC), US-75 (RAP), and US-13 (RPCC) increased with increasing bulk stress due to the stress-hardening behavior of coarse-grained materials, the MR values of US-30 (SG) and US-61 (SG) decreased with increasing bulk stress due to the stress-softening behavior of fine-grained materials. Among US-52 (RAP & RPCC), US-75 (RAP), and US-13 (RPCC), US-75 (RAP) provided the highest MR values, while US-13 (RPCC) showed the lowest SMR values. In addition, US-30 (SG) yielded higher MR values (at the 6<sup>th</sup> loading sequence) than US-61 (SG).

**Table 2. Summary of lab index properties of the different materials.**

Project	Layer	Material Description	Classification		Gravel (%)	Sand (%)	Fines (%)
			AASHTO	USCS			
Adair 160 <sup>th</sup> Street LFM-LGG27--7X-01	Modified Subbase	Crushed Limestone	A-1-a	GP-GM	50.7	37.2	12.0
Blackhawk US20 NHSX-020-6(71)--3H-07	Granular Subbase	Recycled PCC	A-1-a	GP	74.1	24.3	1.6
	Subgrade treatment (special backfill)	Recycled PCC	A-1-a	GP-GM	58.8	34.4	6.9
	Class 10 Subgrade	Glacial Till subgrade	A-6	CL	4.4	53.1	42.4
Des Moines US61 NHSX-061-2(62)--3H-29	Select Subgrade	Glacial till subgrade	A-6	CL	0.5	44.2	55.3
Des Moines Iowa City Rd L-P103GRADE--73-29	Choke stone Base	Crushed Limestone	A-1-b	GP	48.3	29.7	22.0
	Class 10 Subgrade	Native glacial till with organics	A-6	CL	11.8	21.5	66.6
Hamilton IA 175 IM-035-5(111)133--13-40	Select Subgrade	Glacial till subgrade	A-6	CL	6.2	45.8	48.0
	Modified Subbase	Recycled PCC	A-1-a	GW	65.8	32.0	2.2
Dubuque US52 HSIPX-052-2(120)--3L-31	Modified Subbase	Mixture of recycled PCC and asphalt pavement material	A-1-a	GW	60.3	38.1	1.6
Dubuque US52 NHSX-052-2(121)--3H-31	Modified Subbase	Mixture of recycled PCC and asphalt pavement material	A-1-a	GW	50.5	44.6	4.9
Plymouth US75 NHSX-075-2(96)--3H-75	Subgrade treatment (special backfill)	Recycled asphalt pavement material	A-1-a	GW	52.8	45.4	1.8
Linn US13 NHSX-013-1(53)--3H-57	Granular Subbase	Recycled PCC material	A-1-a	GP-GM	68.7	24.8	6.5
Tama US30 NHSX-030-6(191)--3H-86	Granular Subbase	Virgin crushed limestone	A-1-a	GP	90.3	5.1	4.6
Des Moines US61 NHSX-061-2(68)--3H-29	Granular Subbase	Virgin crushed limestone	A-1-a	GP-GM	71.8	20	8.2
Tama US30 NHSX-030-6(191)--3H-86	Select Subgrade	Glacial till subgrade	A-6	CL	3.8	41.3	54.9



**Table 3. Summary of MR test results.**

Material	Compaction level (%)	Model parameters			Mr (ksi) at the 6 <sup>th</sup> loading sequence	Plastic strain at end of test, $\epsilon_p$ (%)
		$k_1$	$k_2$	$k_3$		
US-52 (RAP & RPCC)	95	1,774	0.60	-0.64	26	0.55
	90	1,479	0.71	-0.78	22	0.80
	85	1,565	0.62	-0.72	22	0.89
US-75 (RAP)	95	1,912	0.54	-0.70	28	0.61
	90	1,932	0.49	-0.81	26	0.91
	85	1,926	0.53	-1.08	25	1.12
US-13 (RPCC)	95	1,022	0.55	-0.27	18	0.10
	90	980	0.63	-0.45	17	0.21
	85	739	0.57	-0.12	13	0.87
US-30 (SG)	95	2,215	0.26	-5.34	12	0.12
	90	1,594	0.37	-3.63	11	0.16
	85	1,215	0.19	-3.69	9	0.49
US-61 (SG)	95	2,213	0.29	-7.71	9	0.16
	90	1,114	0.15	-4.9	7	0.17
	85	1,139	0.14	-4.77	8	0.76

### In Situ Point Testing for Calibration

An experimental plan was developed in collaboration with the Iowa DOT pavement design and construction engineering team to perform field testing to determine mechanistic properties on pavement foundation layers in situ at selected project sites across the State of Iowa. The goal at each site was to perform cyclic APLTs to determine composite resilient modulus ( $M_{r-comp}$ ) properties using a 12 in. diameter loading plate (Figure 4) and perform static APLTs to determine  $k$  values with 30 in. diameter loading plate (Figure 5). A dynamic cone penetrometer (DCP) test was conducted at each test location to determine penetration resistance profile and assess layer thicknesses.

The APLT testing plan summarizing the loading sequences for cyclic and static testing provided in Table 4. Cyclic APLTs involved performing a total of 1,500 loading cycles, which involved a 500 cycle conditioning sequence at 15 psi maximum stress followed by 100 to 250 cycles at 5 to 40 psi maximum stresses. Plate deformations and deflection basin measurements at 2x, 3x, and 4x, the plate radius were obtained for back-calculation of the two-layered  $M_r$  properties for each stress sequence. The average of the last 5 cycles was used for representation of  $M_r$  for each loading sequence. A 0.2 sec load time and a 0.8 sec dwell time was used. Static APLTs were performed following AASHTO T222 (2012), using two loading cycles.

A summary of project locations and testing performed, along with RT mapping is provided in Table 5.

**Table 4. Cyclic and static plate load testing configuration.**

Test Designation	Step	Number of cycles, N	Cyclic Stress, $\sigma_{\text{cyclic}}$ [psi]	Minimum stress, $\sigma_{\text{min}}$ [psi]	Maximum Stress, $\sigma_{\text{max}}$	Plate Configuration/Notes
A [1,100 cycle APLT]	Cond.	500	13	2	15.0	12 in. diameter flat plate with deflection readings at r, 2r, 3r, and 4r from plate center [r = plate radius]. 0.2 second load time and 0.8 second dwell time
	1	100	4	2	6.0	
	2	100	8	2	10.0	
	3	100	13	2	15.0	
	4	150	18	2	20.0	
	5	200	28	2	30.0	
6	250	38	2	40.0		
C [Static APLT]	1	2	NA	NA	15.0	30 in. diameter stacked plate, load applied in 2.5 psi increments



**Figure 4. 12 in. diameter loading plate setup for cyclic APLT [picture taken on 08/28/2019 on Blackhawk US20 NHSX-020-6(71)--3H-07 project site over compacted special backfill material]**

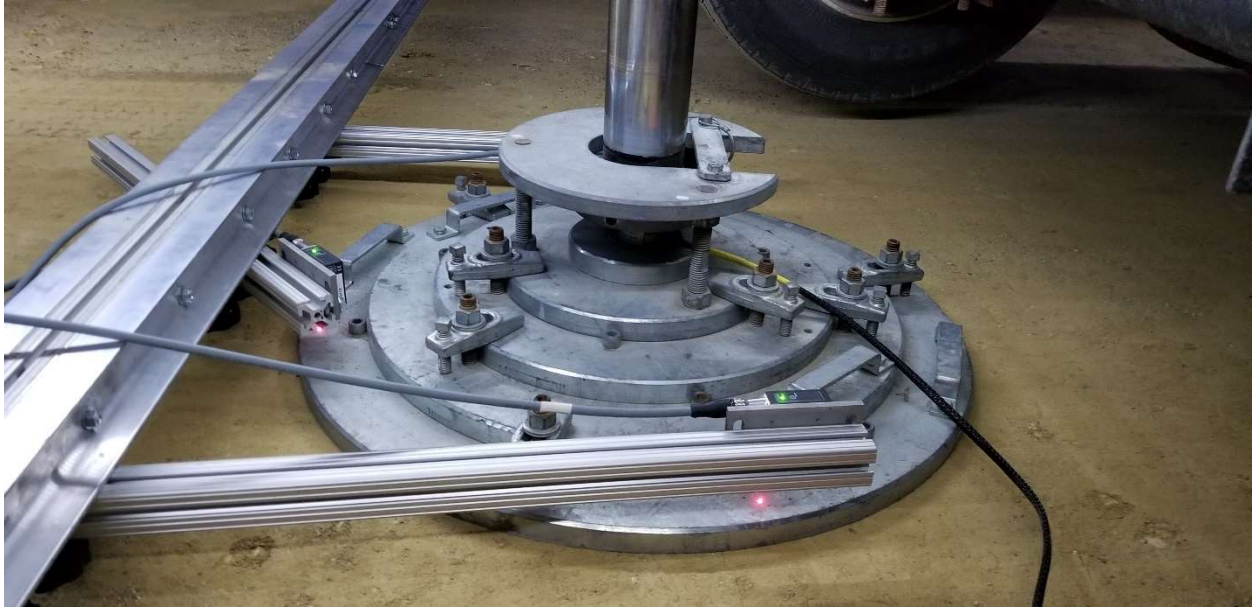


Figure 5. 30 in. diameter loading plate setup for static APLT [picture taken on 10/23/2019 on Des Moines US61 NHSX-061-2(62)--3H-29 project over compacted select subgrade]

Table 5. Summary of project sites, materials, and tests performed.

Project	Layer	Material Description	RT Mapping	APLT Test A	APLT Test B	Vu Meter Tests
Adair 160 <sup>th</sup> Street LFM-LGG27--7X-01	Modified Subbase	Crushed Limestone	5	8 [9/13/2019]	—	—
Blackhawk US20 NHSX-020-6(71)--3H-07	Granular Subbase	Recycled PCC	3	—	8 [8/27/2019 & 9/5/2019]	—
	Subgrade treatment (special backfill)	Recycled PCC	1	10 [8/28/2019]	4 [8/27/2019]	—
	Class 10 Subgrade	Glacial Till subgrade	—	—	—	—
Des Moines US61 NHSX-061-2(62)--3H-29	Select Subgrade	Glacial till subgrade	12	—	9 [10/23/2019]	—
	Modified subbase (haul road)	Crushed Limestone	Included within above maps	—	2 [10/23/2019]	—
Des Moines Iowa City Rd L-P103GRADE--73-29	Choke stone Base	Crushed Limestone	5	—	—	—
	Class 10 Subgrade	Native glacial till with organics	1	—	—	—
Hamilton IA 175	Select Subgrade	Glacial till subgrade	1	—	—	—

IM-035-5(111)133--13-40	Modified Subbase	Recycled PCC	1	10 [9/3/2019]	—	—
Dubuque US52 HSIPX-052-2(120)--3L-31	Modified Subbase	Mixture of recycled PCC and asphalt pavement material	6	10 [9/4/2019]	3 [8/13/2020]	—
Dubuque US20 NHSX-020-9(183)--3H-31	Modified Subbase	Virgin Crushed Limestone	12	—	3 [9/30/2020]	3 [9/30/2020]
	Macadam Base	Virgin Crushed Limestone	4	—	4 [9/25/2020]	—
Dubuque US52 NHSX-052-2(121)--3H-31	Modified Subbase	Mixture of recycled PCC and asphalt pavement material	31	—	—	2 [8/13/2020]
Dubuque US52 NHSX-052-2(121)--3H-31	Subgrade Treatment (Cement treated subgrade)	Cement treated glacial till	3	—	6 [8/12/2020]	—
Plymouth US75 NHSX-075-2(96)--3H-75	Subgrade treatment (special backfill)	Recycled asphalt pavement material	2	—	4 [7/29/2020]	—
	Class 10 Embankment Subgrade	Native Subgrade	1	—	5 [7/28/2020]	—
Linn US13 NHSX-013-1(53)--3H-57	Granular Subbase	Recycled PCC material	12	—	5 [8/20/2020]	3 [8/20/2020]
	Select Subgrade	Glacial Till	—	—	4 [8/21/2020]	—
Tama US30 NHSX-030-6(191)--3H-86	Granular Subbase	Virgin crushed limestone	2	—	11 [7/7/2020 & 7/8/2020]	3 [7/9/2020]
	Select Subgrade	Glacial Till	7	—	6 [6/25/2020 & 6/30/2020]	—
Des Moines US61	Granular Subbase	Virgin crushed limestone	2	—	2 [6/16/2020]	4 [6/16/2020]

NHSX-061-2(68)--3H-29						
Jasper I-80 IM-NHS-080-5(303)174--03-50	Select Subgrade	Glacial till subgrade	2	—	2 [6/18/2020]	—
	Select Treatment (Modified Subbase)	Crushed Limestone	2	—	5 [6/18/2020]	—

## Summary of APLT Results

Example records of APLT results from Test A and Test B are provided in Figure 6 and Figure 7, respectively. All individual test reports are included in Appendix B. No moisture adjustments were made in this study for future changes in saturation levels and those corrections can be applied (AASHTO T222, NCHRP 2000).

The cyclic APLTs were performed to determine stress-dependent  $M_{r-comp}$ . The  $M_r$  constitutive model parameters ( $k_1$ ,  $k_2$ , and  $k_3$ , per AASHTO 2015) were then determined and are presented herein as  $k^*1$ ,  $k^*2$ ,  $k^*3$ , where “\*” is used to differentiate with regression coefficients traditionally developed for laboratory  $M_r$  test measurements. A summary of  $M_{r-comp}$  for the last loading sequence at all test locations along with the test point ID and materials is provided in Table 6.

The static APLTs were used to determine the modulus of subgrade reaction k-value. The k-value is presented herein as  $k_u$  which represents the k value after plate bending correction and with no moisture correction applied, per AASHTO T222 (2012). Two loading/unloading cycles were performed in this study and the results are therefore presented as  $k_{u(1)}$ , and  $k_{u(2)}$  representing values for each loading cycle. If the measurement was performed on top of the granular subbase layer, the  $k_u$  values are presented as  $k_{u(Comp)}$ . The results are presented for a given target stress level of 10 psi, per AASHTO T222. A summary of  $k_{u(1)}$ ,  $k_{u(2)}$ , ratio of  $k_{u(1)}/k_{u(2)}$  and permanent deformation (dp) at the end of the test at all test locations along with the test point ID and materials is provided in Table 7. The k-value measurements are grouped into 4 categories in Table 7, based on calibration analysis and is explained in the following section.

Summary statistics of k-values and  $M_r$ -values are provided in Table 8 and Table 9, respectively.

Permanent or plastic deformation occurring from repeated traffic loading is a recognized cause of pavement distresses. For rigid pavements, increases in total permanent deformation in the unbound layers contribute to increased faulting, roughness, and transverse cracking and reduced load-transfer efficient (LTE). In a study conducted by Birkhoff and McCullough (1979), a void gap of about 0.05 in. can lead to loss of support (LOS), thereby increasing the bending stresses in the pavement leading to fatigue failure. For flexible pavements, as total permanent deformation within unbound and subgrade layers increases, surface rutting, roughness, and cracking increase. It is

therefore essential that permanent deformation be measured, and mechanistic-empirical models developed to predict permanent deformation performance.

Permanent deformations ( $\delta_p$ ) were monitored during cyclic and static APLTs conducted for this project. A summary of  $\delta_p$  values from static PLTs is provided in Table 8. Figure 8 provides a graph of  $k_{u(1)}$  versus  $\delta_p$  from static APLT results at all project sites, which shows a strong power relationship between the two parameters. Based on this relationship, to limit  $\delta_p$  to a critical 0.05 in., a minimum  $k_{u(1)} = 200$  pci must be achieved. Further, the results indicated that 63 out of the 100 measurements obtained from this project showed k-values less than the assumed value of 150 pci.

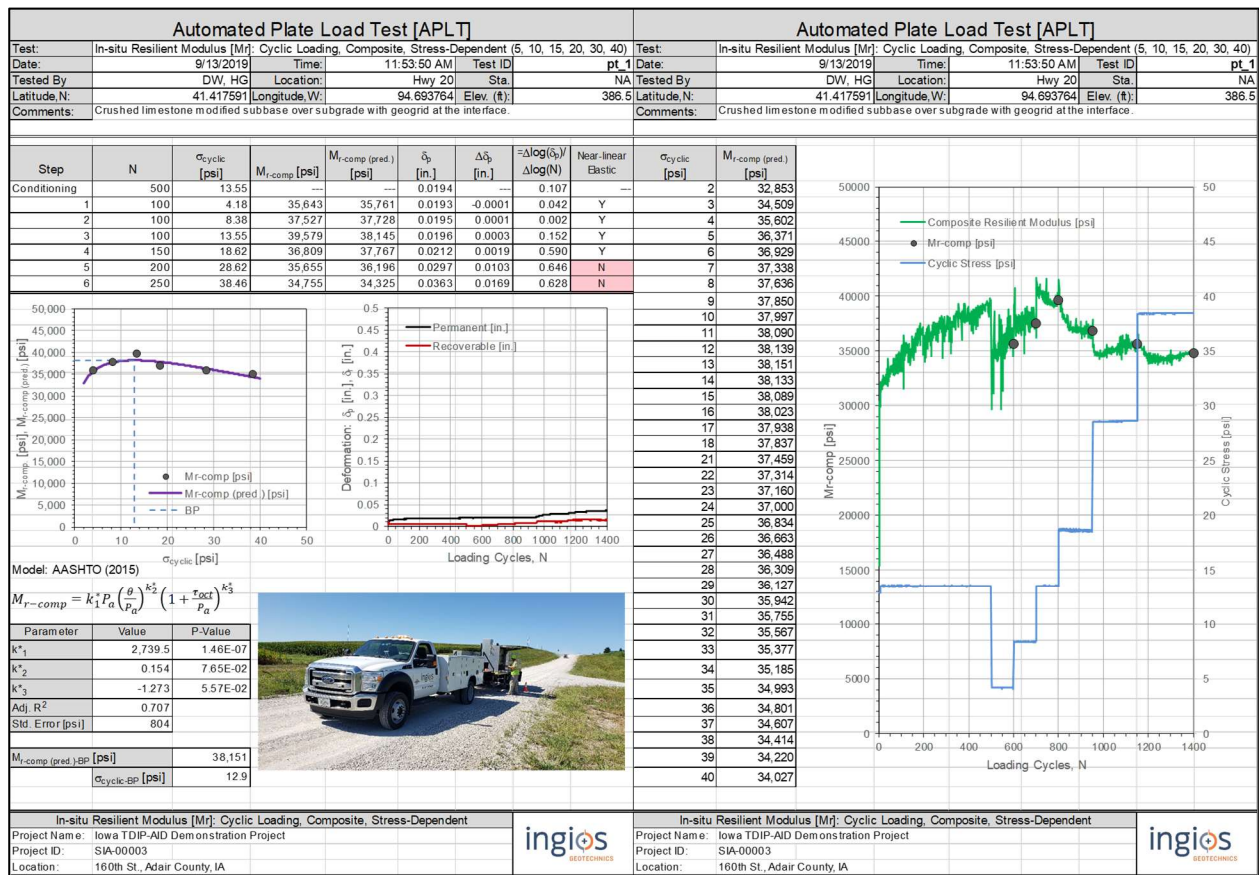


Figure 6. Example APLT data record showing 12 in. static plate load test results (Test A)

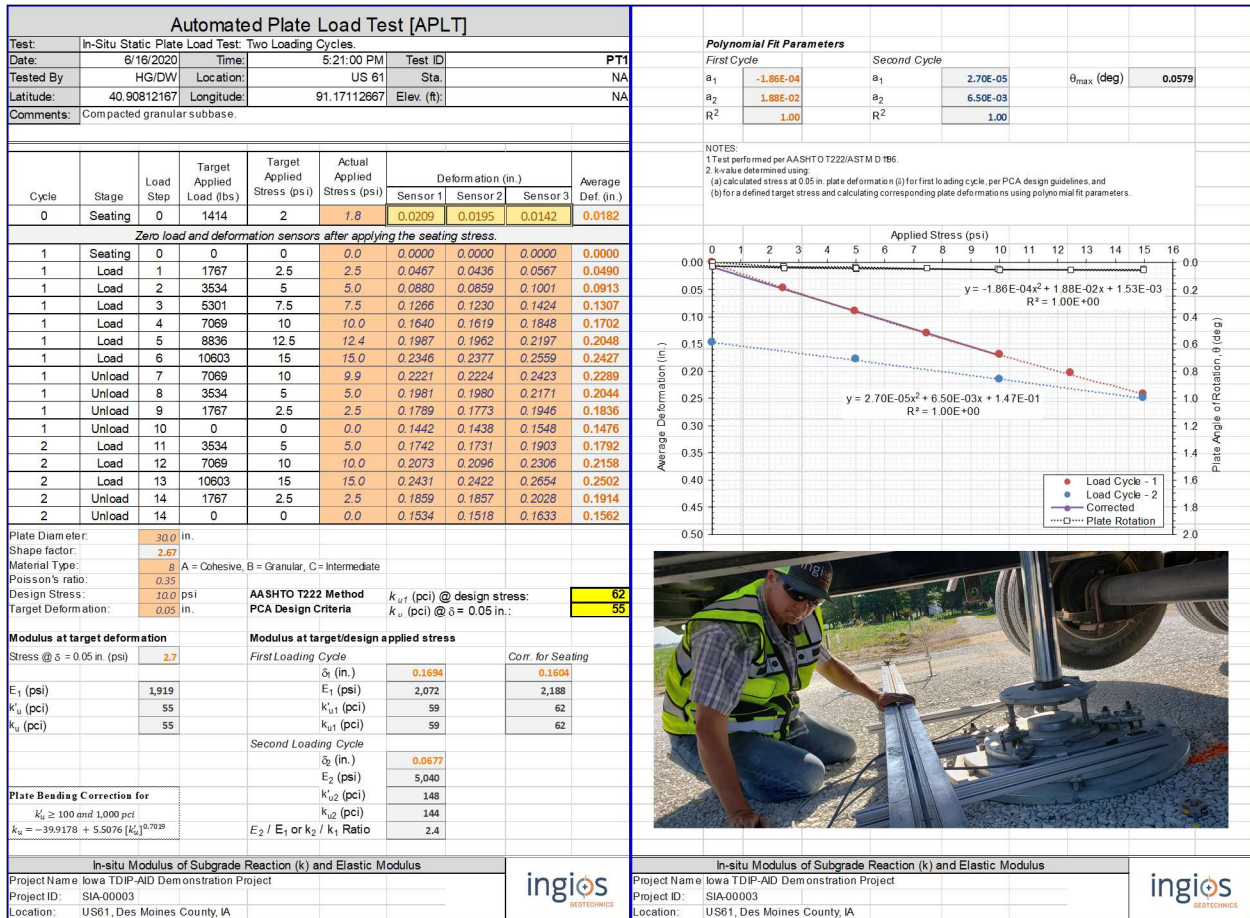


Figure 7. Example APLT data record showing 30 in. static plate load test results (Test A)

Table 6. Summary of APLT results (Test A)

Date	Point	Material	$M_r$ -comp (psi)
8/28/2019	Hwy20_pt_11	RPCC special backfill layer over subgrade.	14,593
8/28/2019	Hwy20_pt_12	RPCC special backfill layer over subgrade.	17,997
8/28/2019	Hwy20_pt_13	RPCC special backfill layer over subgrade.	20,389
8/28/2019	Hwy20_pt_14	RPCC special backfill layer over subgrade.	21,427
8/28/2019	Hwy20_pt_15	RPCC special backfill layer over subgrade.	24,342
8/28/2019	Hwy20_pt_16	RPCC special backfill layer over subgrade.	15,871
8/28/2019	Hwy20_pt_17	RPCC special backfill layer over subgrade.	16,101
8/28/2019	Hwy20_pt_18	RPCC special backfill layer over subgrade.	18,282
8/28/2019	Hwy20_pt_19	RPCC special backfill layer over subgrade.	15,082
8/28/2019	Hwy20_pt_20	RPCC special backfill layer over subgrade.	23,770
9/4/2019	Hwy52_pt_1	Crushed limestone modified subbase over subgrade.	25,464
9/4/2019	Hwy52_pt_2	Crushed limestone modified subbase over subgrade.	37,271
9/4/2019	Hwy52_pt_3	Crushed limestone modified subbase over subgrade.	55,945
9/4/2019	Hwy52_pt_4	Crushed limestone modified subbase over subgrade.	52,216
9/4/2019	Hwy52_pt_5	Crushed limestone modified subbase over subgrade.	9,217
9/4/2019	Hwy52_pt_6	Crushed limestone modified subbase over subgrade.	5,609
9/4/2019	Hwy52_pt_7	Crushed limestone modified subbase over subgrade.	24,784
9/4/2019	Hwy52_pt_8	Crushed limestone modified subbase over subgrade.	31,756

9/4/2019	Hwy52_pt_9	Crushed limestone modified subbase over subgrade.	26,848
9/4/2019	Hwy52_pt_10	Crushed limestone modified subbase over subgrade.	31,374
9/3/2019	Hwy175_pt_1	Recycled Aggregate modified subbase over subgrade.	29,440
9/3/2019	Hwy175_pt_2	Recycled Aggregate modified subbase over subgrade.	12,567
9/3/2019	Hwy175_pt_3	Recycled Aggregate modified subbase over subgrade.	13,250
9/3/2019	Hwy175_pt_4	Recycled Aggregate modified subbase over subgrade.	15,953
9/3/2019	Hwy175_pt_5	Recycled Aggregate modified subbase over subgrade.	29,984
9/3/2019	Hwy175_pt_6	Recycled Aggregate modified subbase over subgrade.	26,062
9/3/2019	Hwy175_pt_7	Recycled Aggregate modified subbase over subgrade.	25,111
9/3/2019	Hwy175_pt_8	Recycled Aggregate modified subbase over subgrade.	17,782
9/3/2019	Hwy175_pt_9	Recycled Aggregate modified subbase over subgrade.	20,322
9/3/2019	Hwy175_pt_10	Recycled Aggregate modified subbase over subgrade.	17,858
9/13/2019	160th St_pt_1	Crushed limestone modified subbase over subgrade with geogrid at the interface.	34,325
9/13/2019	160th St_pt_2	Crushed limestone modified subbase over subgrade with geogrid at the interface.	32,436
9/13/2019	160th St_pt_3	Crushed limestone modified subbase over subgrade with geogrid at the interface.	32,564
9/13/2019	160th St_pt_4	Crushed limestone modified subbase over subgrade with geogrid at the interface.	28,320
9/13/2019	160th St_pt_5	Crushed limestone modified subbase over subgrade with geogrid at the interface.	26,762
9/13/2019	160th St_pt_6	Crushed limestone modified subbase over subgrade with geogrid at the interface.	22,532
9/13/2019	160th St_pt_7	Crushed limestone modified subbase over subgrade with geogrid at the interface.	28,894
9/13/2019	160th St_pt_8	Crushed limestone modified subbase over subgrade with geogrid at the interface.	5,880

**Table 7. Summary of APLT results (Test B)**

Date	Test Point	Material ID	k <sub>u1</sub> (pci)	k <sub>u2</sub> (pci)	Ratio	δ <sub>p</sub> at end of test (in.)
9/30/2020	Hwy20_pt1	Modified Subbase - Crushed limestone.	129.6	388.7	3.0	0.088
9/30/2020	Hwy20_pt3	Modified Subbase - Crushed limestone.	153.6	341.5	2.2	0.075
9/30/2020	Hwy20_pt5	Modified Subbase - Crushed limestone.	176.9	361.9	2.0	0.066
8/13/2020	US52_pt1	Modified Subbase material consisting of a mixture of Recycled PCC & RAP	69.4	168.9	2.4	0.162
8/13/2020	US52_pt2	Modified Subbase material consisting of a mixture of Recycled PCC & RAP	135.5	626.0	4.6	0.118
8/13/2020	US52_pt4	Modified Subbase material consisting of a mixture of Recycled PCC & RAP	92.9	249.1	2.7	0.126
7/29/2020	Hwy75_pt1	Compacted special backfill.	60.6	158.8	2.6	0.183
7/29/2020	Hwy75_pt3	Compacted special backfill.	20.4	69.0	3.4	0.571
7/29/2020	Hwy75_pt4	Compacted special backfill.	44.3	110.3	2.5	0.257
7/29/2020	Hwy75_pt5	Compacted special backfill.	111.9	369.0	3.3	0.104



8/27/2019	Hwy20_pt7	Recycled PCC special backfill over subgrade.	67.7	219.8	3.2	0.179
8/27/2019	Hwy20_pt8	Recycled PCC special backfill over subgrade.	152.6	318.2	2.1	0.066
8/27/2019	Hwy20_pt9	Recycled PCC special backfill over subgrade.	118.1	268.0	2.3	0.086
8/27/2019	Hwy20_pt10	Recycled PCC special backfill over subgrade.	128.9	267.5	2.1	0.077
10/23/2019	US61, pt9	Aggregate subbase over compacted subgrade.	188.5	451.0	2.4	0.063
10/23/2019	US61, pt10	Aggregate Base (access road) over compacted subgrade (Select)	138.0	372.0	2.7	0.089
8/12/2020	US52_pt1	Cement Stabilized subgrade	173.9	248.9	1.4	0.037
8/12/2020	US52_pt2	Cement Stabilized Subgrade	190.9	286.3	1.5	0.034
8/12/2020	US52_pt3	Cement Stabilized Subgrade	237.3	403.6	1.7	0.028
8/12/2020	US52_pt4	Compacted select subgrade.	112.2	276.8	2.5	0.094
8/12/2020	US52_pt5	Compacted select subgrade.	127.9	301.6	2.4	0.084
8/12/2020	US52_pt6	Cement Stabilized Subgrade, over culvert	371.4	884.9	2.4	0.025
6/18/2020	I80_pt1	Compacted subgrade - Area compacted on 06/10, per contractor. Material wet and visible rutting.	48.8	120.2	2.5	0.203
6/18/2020	I80_pt2	Compacted subgrade - Area compacted with a sheepsfoot roller, dry crust near the surface, and experienced	36.2	101.0	2.8	0.299
8/21/2020	US13, pt1	Subgrade-Select	259.0	413.1	1.6	0.035
8/21/2020	US13, pt2	Subgrade-Select	335.1	581.6	1.7	0.029
8/21/2020	US13, pt3	Subgrade-Select	231.7	729.1	3.1	0.043
8/21/2020	US13, pt4	Subgrade-Select	125.3	303.7	2.4	0.084
7/28/2020	Hwy75_pt1	Compacted Select Subgrade.	209.3	350.1	1.7	0.036
7/28/2020	Hwy75_pt2	Compacted Select Subgrade.	183.1	294.7	1.6	0.044
7/28/2020	Hwy75_pt3	Compacted Select Subgrade.	208.9	342.3	1.6	0.035
7/28/2020	Hwy75_pt4	Compacted Select Subgrade.	219.9	336.0	1.5	0.027
7/28/2020	Hwy75_pt5	Compacted Select Subgrade.	142.5	244.1	1.7	0.061
6/25/2020	US30A_pt3	Compacted Subgrade.	145.1	296.3	2.0	0.076
6/30/2020	US30B_pt1	Compacted subgrade.	72.5	165.9	2.3	0.146
6/30/2020	US30B_pt2	Compacted subgrade.	220.2	392.3	1.8	0.038
6/30/2020	US30B_pt3	Compacted subgrade.	175.0	411.7	2.4	0.057
6/30/2020	US30B_pt4	Compacted subgrade.	104.4	252.9	2.4	0.103
6/30/2020	US30B_pt5	Compacted subgrade.	110.4	227.1	2.1	0.098
10/23/2019	US61_pt1	Compacted Subgrade (Select)	155.8	336.3	2.2	0.067
10/23/2019	US61_pt2	Compacted Subgrade (Select)	209.7	472.6	2.3	0.038
10/23/2019	US61_pt3	Compacted Subgrade (Select)	232.7	524.4	2.3	0.035
10/23/2019	US61_pt4	Compacted Subgrade (Select)	226.2	474.7	2.1	0.041
10/23/2019	US61_pt5	Compacted Subgrade (Select)	239.5	527.0	2.2	0.037

10/23/2019	US61_pt6	Compacted Subgrade (Select)	123.6	306.5	2.5	0.091
10/23/2019	US61_pt7	Compacted Subgrade (Select)	161.2	352.5	2.2	0.051
10/23/2019	US61_pt8	Compacted Subgrade (Select)	214.4	427.1	2.0	0.036
10/24/2019	US61_pt11	Compacted Subgrade (Select)	82.5	220.9	2.7	0.114
6/16/2020	US61_pt1	Compacted granular subbase.	62.3	143.6	2.3	0.156
6/16/2020	US61_pt3	Compacted granular subbase.	129.0	265.9	2.1	0.087
9/25/2020	US20_pt1	Macadam Stone Base	72.5	357.0	4.9	0.210
9/25/2020	US20_pt2	Macadam Stone Base	98.2	339.9	3.5	0.132
9/25/2020	US20_pt3	Macadam Stone Base	69.6	210.6	3.0	0.180
9/25/2020	US20_pt4	Macadam Stone Base	106.9	362.6	3.4	0.141
7/7/2020	US30_pt1	Compacted Granular Subbase - One vibratory roller mapping pass.	119.5	336.5	2.8	0.108
7/7/2020	US30_pt2	Compacted Granular Subbase - One vibratory roller mapping pass.	90.8	230.1	2.5	0.124
7/7/2020	US30_pt3	Compacted Granular Subbase - One vibratory roller mapping pass.	115.1	359.3	3.1	0.111
7/7/2020	US30_pt4	Compacted Granular Subbase - One vibratory roller mapping pass.	123.4	347.9	2.8	0.104
7/7/2020	US30_pt5	Compacted Granular Subbase - One vibratory roller mapping pass.	156.9	372.8	2.4	0.077
7/8/2020	US30_pt8	Compacted Granular Subbase - Test performed after eight vibratory roller passes.	136.7	310.3	2.3	0.084
7/8/2020	US30_pt9	Compacted Granular Subbase - Test performed after eight vibratory roller passes.	154.3	362.3	2.3	0.076
7/8/2020	US30_pt10	Compacted Granular Subbase - Test performed after sixteen vibratory roller passes.	153.1	349.3	2.3	0.088
7/8/2020	US30_pt11	Compacted Granular Subbase - Test performed after sixteen vibratory roller passes.	144.7	361.9	2.5	0.078
7/8/2020	US30_pt12	Compacted Granular Subbase - Test performed after sixteen vibratory roller passes.	141.2	358.2	2.5	0.082
7/8/2020	US30_pt13	Compacted Granular Subbase - Test performed after eight vibratory roller passes.	104.5	252.6	2.4	0.114
8/27/2019	US20_pt1_2019	Recycled PCC granular subbase over special backfill and subgrade.	92.2	292.4	3.2	0.135
8/27/2019	US20_pt2_2019	Recycled PCC granular subbase over special backfill and subgrade.	81.9	280.5	3.4	0.158
8/27/2019	US20_pt3_2019	Recycled PCC granular subbase over special backfill and subgrade.	87.6	289.6	3.3	0.148
9/5/2019	US20_pt21_2019	Recycled PCC granular subbase over special backfill and subgrade.	111.5	380.0	3.4	0.115
9/5/2019	US20_pt22_2019	Recycled PCC granular subbase over special backfill and subgrade.	122.2	458.2	3.7	0.114
9/5/2019	US20_pt23_2019	Recycled PCC granular subbase over special backfill and subgrade.	154.6	454.6	2.9	0.077
9/5/2019	US20_pt24_2019	Recycled PCC granular subbase over special backfill and subgrade.	140.5	449.6	3.2	0.087

9/5/2019	US20_pt25_2019	Recycled PCC granular subbase over special backfill and subgrade.	91.3	334.0	3.7	0.141
6/18/2020	I80_PT3	Reworked subgrade with nominal 24 inches thick granular treatment over clay subgrade, with biaxial geogrid	166.3	312.0	1.9	0.074
6/18/2020	I80_PT4	Reworked subgrade with nominal 24 inches thick granular treatment over clay subgrade, with biaxial geogrid	153.7	302.9	2.0	0.078
6/18/2020	I80_PT5	Reworked subgrade with nominal 24 inches thick granular treatment over clay subgrade, with biaxial geogrid	202.2	393.1	1.9	0.057
6/18/2020	I80_PT6	Reworked subgrade with nominal 24 inches thick granular treatment over clay subgrade, with biaxial geogrid	171.9	422.8	2.5	0.085
6/18/2020	I80_PT7	Reworked subgrade with granular treatment over clay subgrade, with biaxial geogrid at the interface.	93.2	186.2	2.0	0.094
8/20/2020	US13_PT1	Granular Subbase - Recycled PCC	175.1	551.4	3.1	0.097
8/20/2020	US13_PT2	Granular Subbase - Recycled PCC	59.8	206.0	3.4	0.199
8/20/2020	US13_PT3	Granular Subbase - Recycled PCC	55.7	175.0	3.1	0.205
8/20/2020	US13_PT4	Granular Subbase - Recycled PCC	99.6	327.9	3.3	0.132
8/20/2020	US13_PT5	Granular Subbase - Recycled PCC	119.6	438.7	3.7	0.118

Material Group ID: k-St-So

Material Group ID: k-SG

Material Group ID: k-So-So

Material Group ID: k-St-St

**Table 8. Summary of k-value test results.**

Material Group ID	No. of Tests	Minimum (pci)	Maximum (pci)	Average (pci)	Std. Deviation (pci)	COV (%)
k-St-So	16	20.4	188.5	111.8	123.5	48.4
k-SG	32	36.2	371.4	177.7	179.1	75.1
k-So-So	25	62.3	156.9	114.4	115.1	28.8
k-St-St	10	55.7	202.2	129.7	136.7	51.3

**Table 9. Summary of  $M_{r-comp}$  (at 40 psi maximum stress) value test results.**

No. of Tests	Minimum (pci)	Maximum (pci)	Average (pci)	Std. Deviation (pci)	COV (%)
38	5,609	55,945	23,905	24,056	10,608

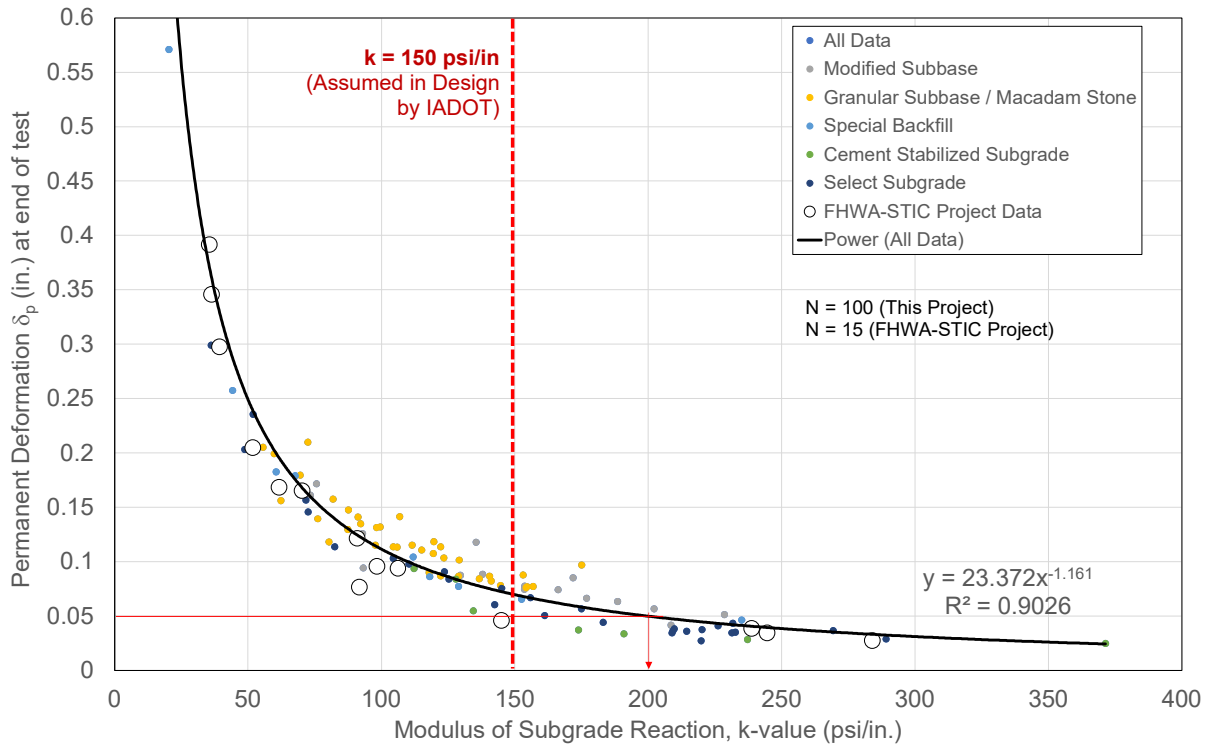


**Figure 8. k-value versus permanent deformation ( $\delta_p$ ) at the end of test from field test measurements at all project sites**

## Calibration Analysis Results

COMP-Score RT calibration records showing the measured versus predicted  $M_{r-comp}$  and k-values are provided in Figure 9 to Figure 13.  $M_{r-comp}$  value calibration analysis was performed on measurements obtained from a few sites on granular materials. k-value calibration analysis was performed on materials with varying profiles and stiffnesses across the state, which provided four unique trends. These trends are related to the following material groups and are identified with a unique calibration model ID as follows:

1. IA-AID\_k-SG – cohesive subgrade materials (cement treated/untreated)
2. IA-AID\_k-So-So – granular subbase materials over untreated cohesive subgrade
3. IA-AID\_k-St-So – modified subbase or special backfill materials over subgrade.
4. IA-AID\_k-St-St – relatively stiff layer of modified subbase or granular subbase with CBR > 10 over relatively stiff underlying subgrade layer.

A summary of the regression statistics and the measurement validity range for each measurement value for each model is included in Figure 9 to Figure 13, and the regression statistics for all the models are summarized in Table 10. Regression relationships yielded  $R^2$  values ranging between 0.92 and 0.94 representing strong correlations and high confidence in the predicted values.

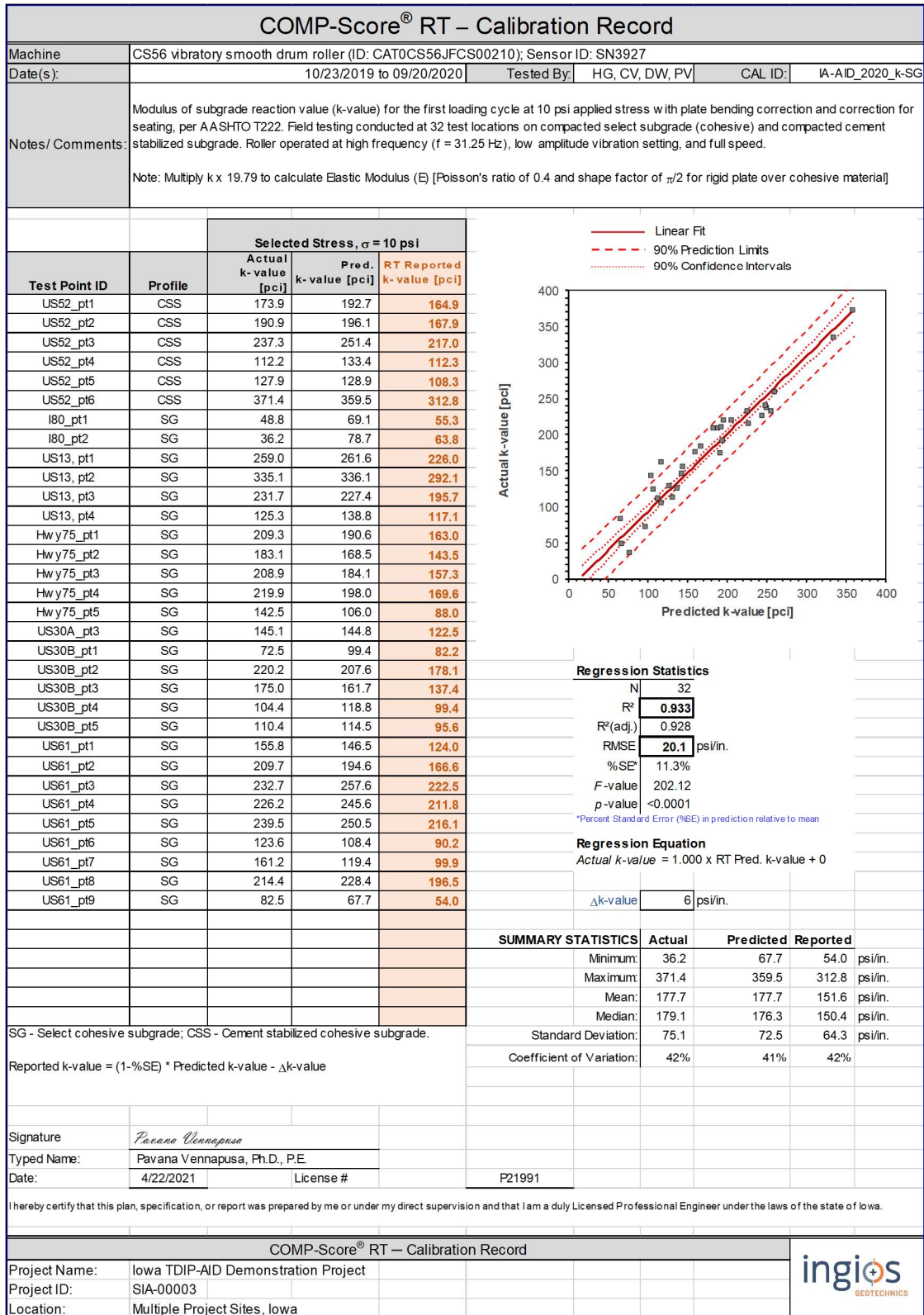


**Figure 9. Calibration record for treated/untreated subgrade materials (Model ID: IA-AID\_2020\_k-SG)**

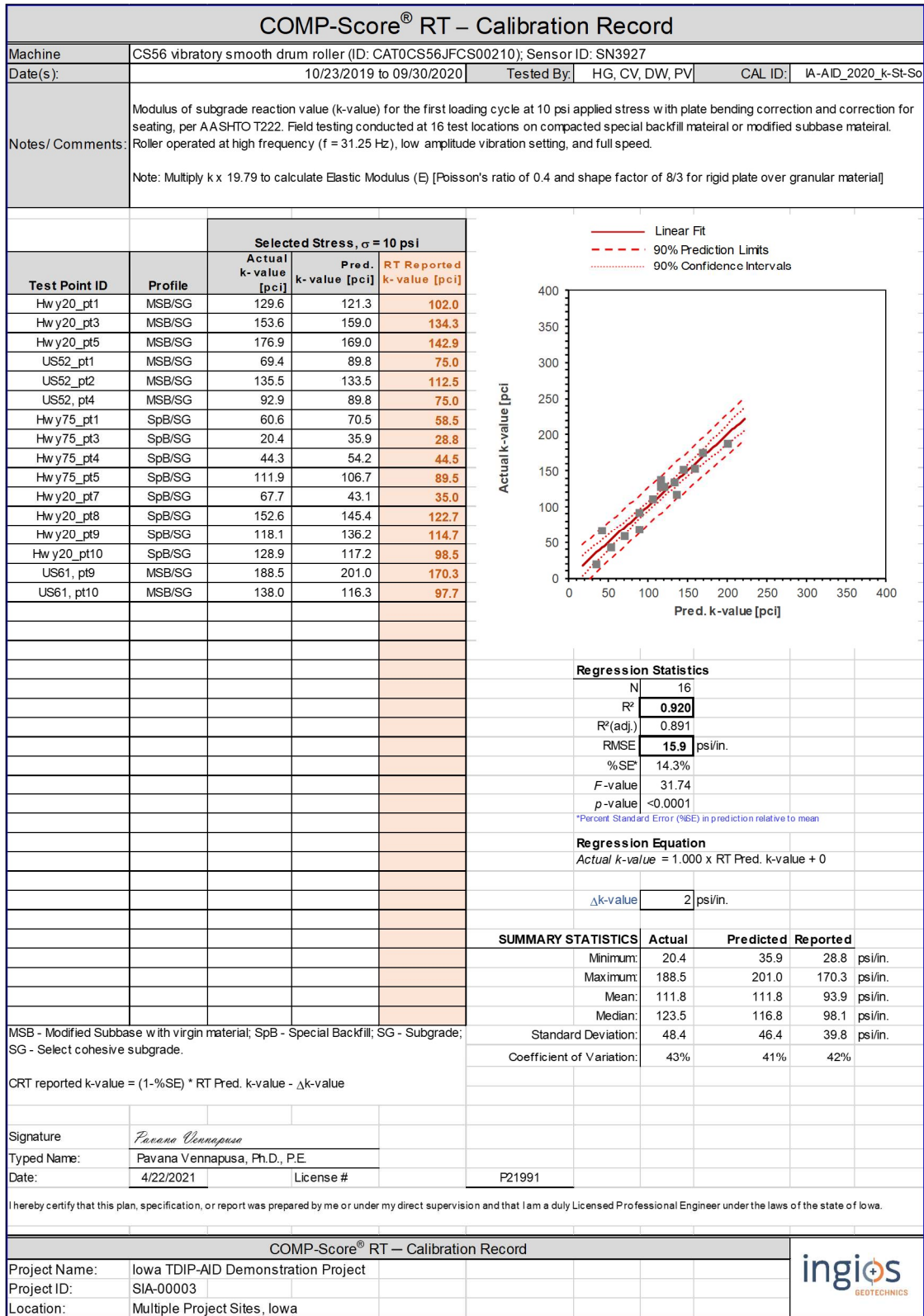


**Figure 10. Calibration record for modified subbase or special backfill top layer underlain by subgrade layers (Model ID: IA-AID\_2020\_k-St-So)**

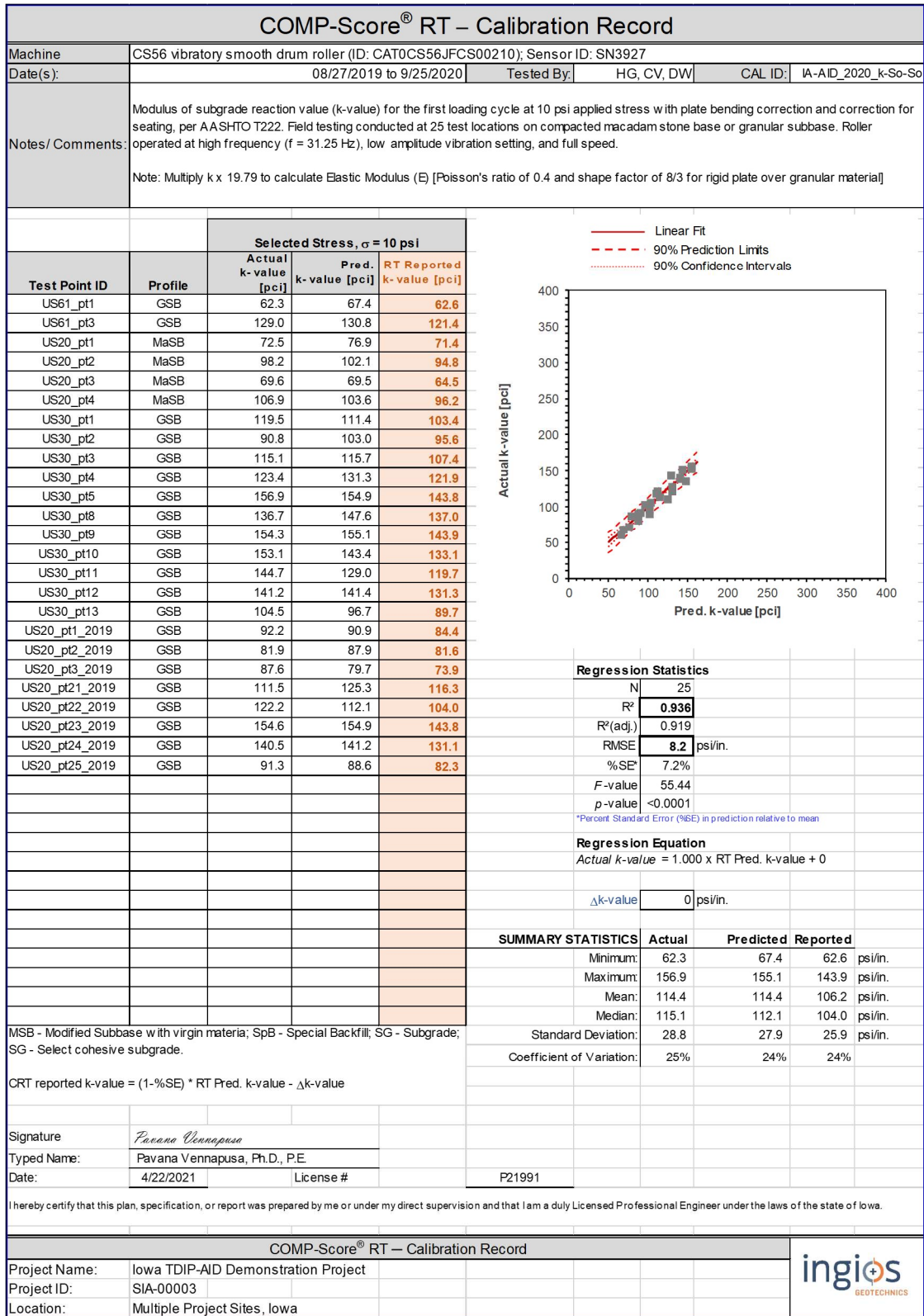


**Figure 11. Calibration record for granular subbase over soft underlying subgrade layers (Model ID: IA-AID\_2020\_k-So-So)**





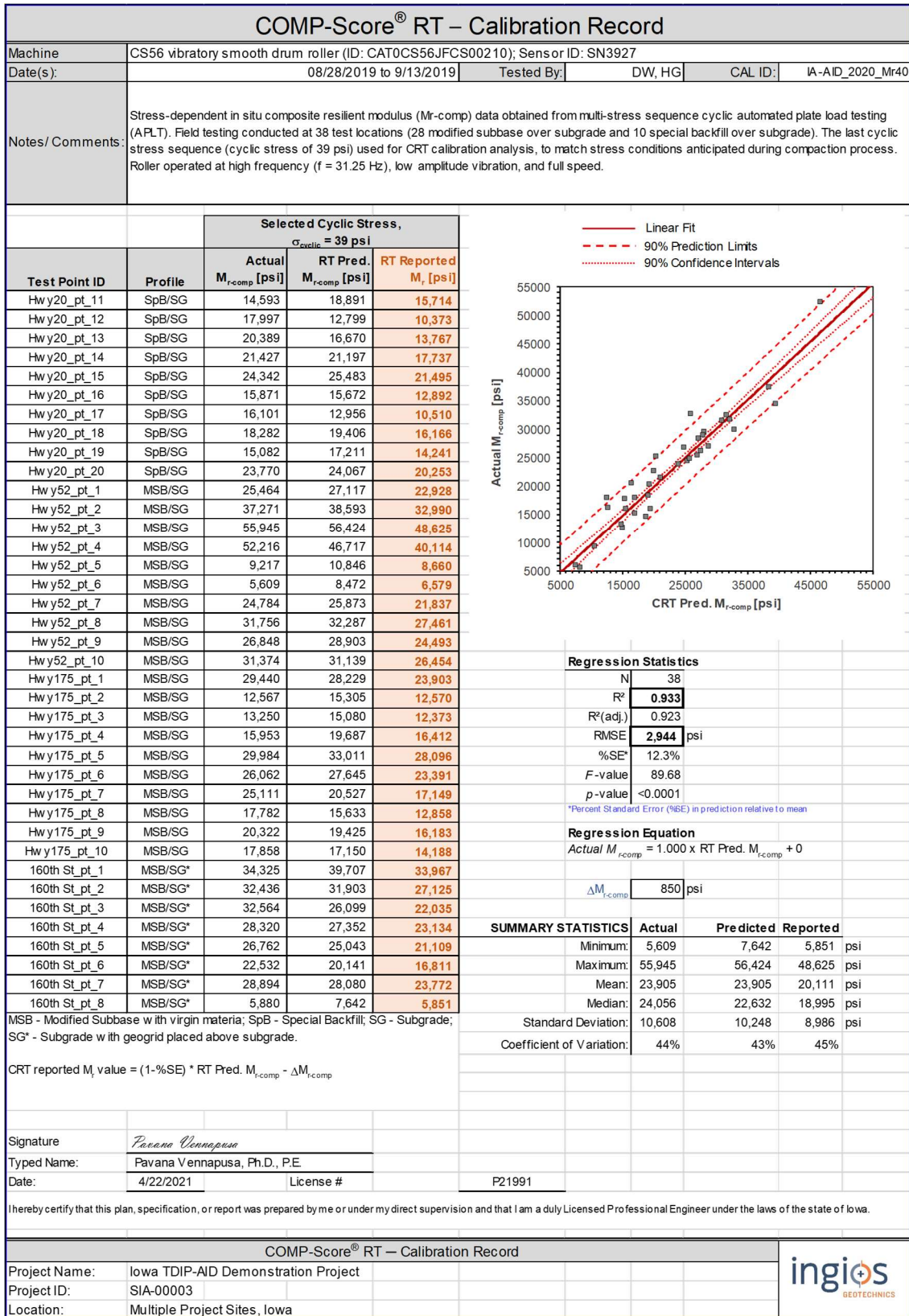


Figure 13. Calibration record for granular materials (Model ID: IA-AID\_2020\_Mr40)

**Table 10. Summary of calibration model regression statistics.**

Parameter	Model ID				
	IA-AID_2020_Mr40	IA-AID_2020_k-St-So	IA-AID_2020_k-SG	IA-AID_2020_k-So-So	IA-AID_2020_k-St-St
N	38	16	32	25	10
R <sup>2</sup>	0.933	0.920	0.933	0.936	0.944
R <sup>2</sup> (adj.)	0.923	0.891	0.928	0.919	0.937
RMSE	2,944	15.9	20.1	8.2	12.9
%SE*	12.3%	14.3%	11.3%	7.2%	9.9%
F-value	89.68	31.74	202.12	55.44	135.04
p-value	<0.0001	<0.0001	<0.0001	<0.0001	<0.0001

### Mapping Results and e-Compaction Reports

A total of 115 COMP-Score RT maps were obtained from all the project sites. The number of maps for each material type from each project site is summarized in Table 7. All e-Compaction reports generated for this project are included in Appendix C. A few highlights are presented below with a k-value map from the US20 project for granular subbase and special backfill material in Figure 14 and Mr-comp map on modified subbase and subgrade material in Figure 15.

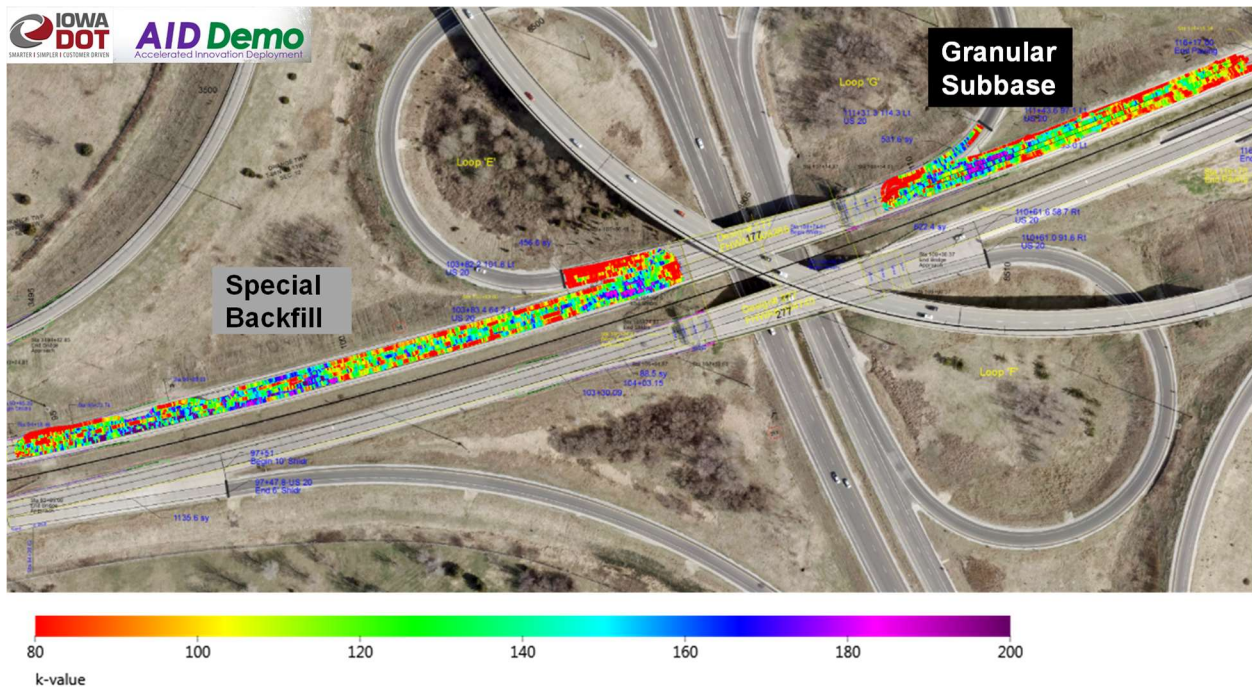


**Figure 14. k-value map on granular subbase and special backfill subgrade treatment layers on Blackhawk County US20 project (08/27/2019)**

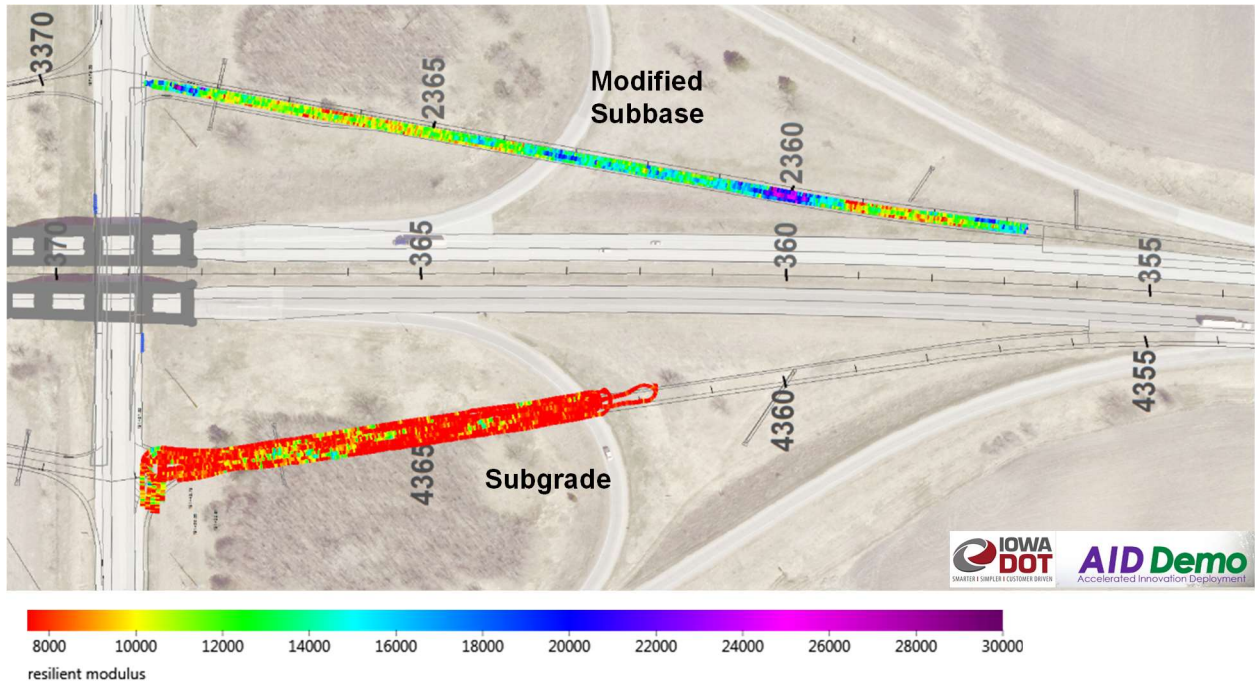


Figure 15.  $M_{r-comp}$  map on modified subbase and embankment subgrade Class 10 material on Hamilton County I-35/Hwy 175 project.

## **Vu Meter Drainage Test Results**

Iowa DOT specifications for granular subbase construction require compaction using static roller passes and no vibration is allowed due to particle breakage and the resulting effect on drainage. Field testing was conducted using the Vu meter provided by the Iowa DOT to assess relative drainage times on subbase layers after different compaction passes. This testing was performed in selected sections at a few project sites with 1 to 24 vibratory roller passes. Testing was performed on both granular subbase and modified subbase materials.

Pictures from testing are included in Figure 16 to Figure 18. Results from the testing are summarized in Table 11 and Figure 19.

Per John Hart, PCC Field Engineer, Iowa DOT, if the time taken to fully drain the way in the Vu meter is between 30 and 120 seconds, the section is considered to provide “good” drainage. Results indicated that all granular subbase test sections showed  $\leq 12$  seconds to fully drain the water, after 1 to 24 vibratory roller compaction passes.

The drainage time in the modified subbase layer test sections ranged between 86 and 261 seconds.



**Figure 16. Vu meter testing on crushed limestone granular subbase on Des Moines County US61 project (06/16/2020).**



**Figure 17. Vu meter testing on crushed limestone granular subbase on Tama County US30 (07/09/2020).**



**Figure 18. Vu meter testing on crushed limestone modified subbase on Dubuque County US20 project (09/30/2020).**

**Table 11. Summary of Vu meter test results from multiple project sites.**

Date	Location	Material	No. of Vibratory Roller Passes	No. of Tests	Vu Drainage Meter – Time for Drainage (sec)		
					Minimum	Maximum	Average
6/16/2020	US61, Des Moines County, IA	Granular Subbase (4121) Crushed Limestone	3	1	12		12
			5	3	9	10	9
			8	1	12		12
			12	2	9	11	10
7/9/2020	US30, Tama County, IA	Granular Subbase (4121) Crushed Limestone	1	7	9	14	11
			8	3	8	9	8
			24	3	9	12	10
8/20/2020	US13, Linn County, IA	Granular Subbase (4121) Recycled Concrete	1	2	9	10	9
			8	1	11		11
			24	2	9	11	10
8/13/2020	US52, Dubuque County, IA	Modified Subbase (4123) Mixture of Recycled PCC and RAP	1	3	108	220	148
			16	2	101	261	181
9/30/2020	US20, Dubuque County, IA	Modified Subbase (4123) Crushed Limestone	1	2	149	153	151
			8	1	86		86
			24	2	95	111	103



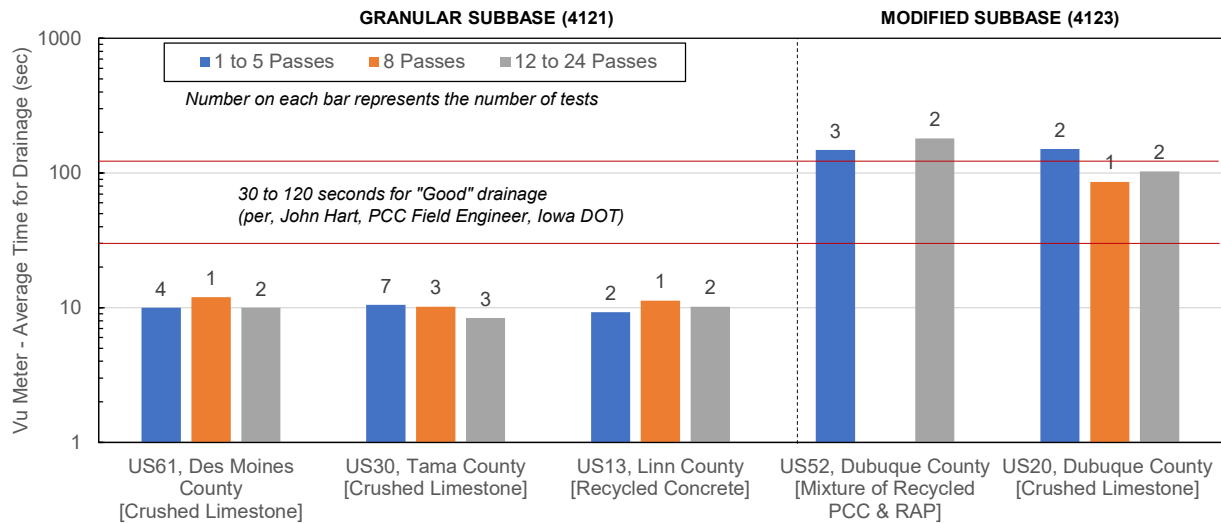


**Figure 19. Bar chart of Vu meter test results form multiple project sites.**

### Design Life Prediction Analysis

The RT mapping results showing geospatial record of k-values allows for design life prediction analysis. To illustrate this possibility, k-value mapping results form the Blackhawk County US20 project are shown in Figure 20 and the predicted design life values are shown in Figure 21. Both these maps are shown as delta maps with a reference target value as noted in the figures.

The design life was calculated using the AASHTO (1993) rigid pavement design model using the design loading conditions (ESALs) assumed for the project by the Iowa DOT and other input parameters are noted in Figure 21, and applying a reduction in the k-value for a LOS condition. An LOS = 2 was assumed (per AASHTO 1993), because of the potential void gap at locations with > 0.05 inch permanent deformation. This was determined using the empirical relationship between k-value and  $\delta_p$  from static APLTs (Figure 8), and all grid point locations on the map with k-value < 200 pci was corrected for the LOS condition.

Results indicated a 20% to 25% decrease in assumed pavement design life as an impact of the foundation support conditions. This has significant cost implications in terms of potential maintenance work and safety impacts to public and construction works due to road closures.

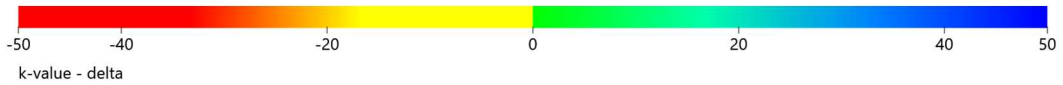
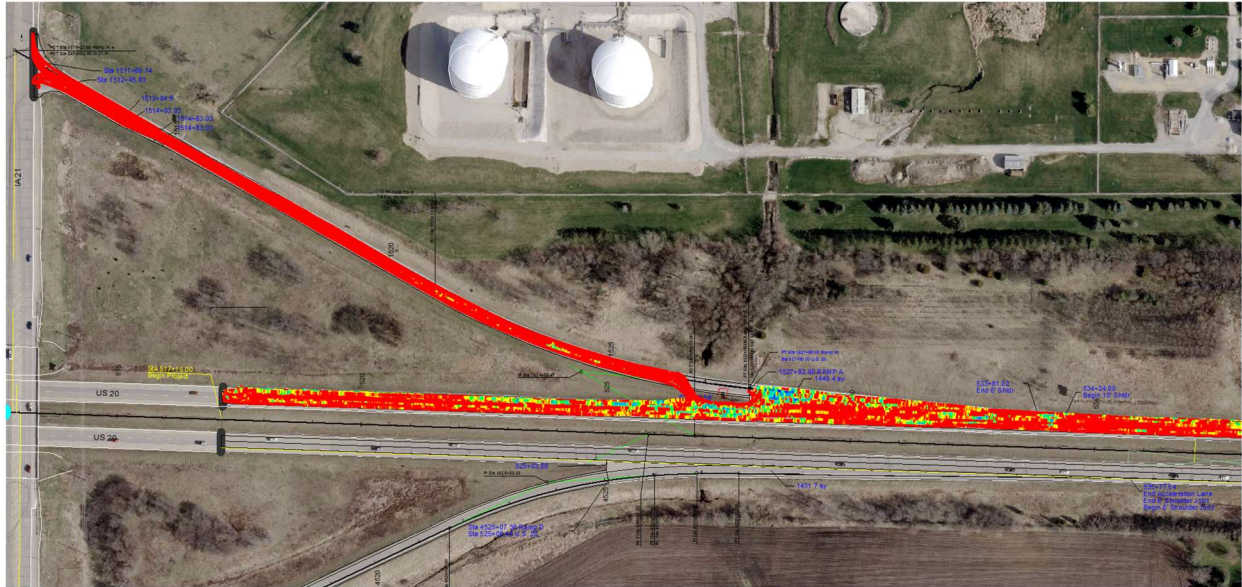


**Figure 20. Delta k-value map (assuming a target k-value of 150 pci) of granular subbase layer on Blackhawk US20 project (08/27/2020).**

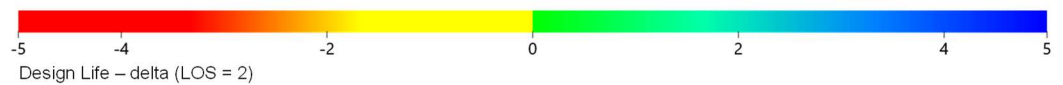
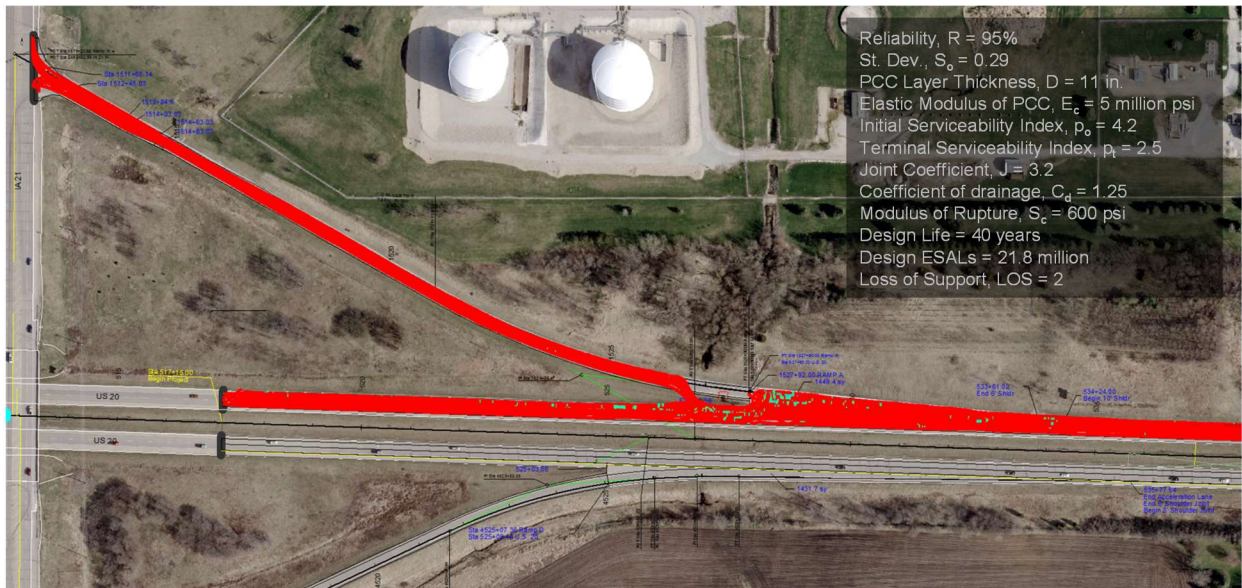


**Figure 21. Predicted delta design life map (assumed target design life = 40 years) per AASHTO (1993) pavement design assuming LOS = 2.**

## References

Dupont, W.D., Plummer, W.D. (1998). "Power and sample size calculations for studies involving linear regression," *Controlled Clinical Trails*, Vol. 19, 589-601.

Tutumluer, E., Moaveni, M., White, D.J., and Vennapusa, P. (2018). "Validation of intelligent compaction to characterize pavement foundation mechanical properties," Research Report No: UILU-ENG-2018, Sponsored by the Illinois State Toll Highway Authority, Submitted by University of Illinois at Urbana-Champaign, Champaign, IL.

White, D.J., Vennapusa, P., Cackler, T. (2014). "ICM Report – Ohio River Bridges East End Crossing I-265, Section 6, Sta. 350+00 to 400+00", Report submitted for Walsh Vinci Construction, Inc., by Ingios Geotechnics, Inc. (unpublished report).

White, D.J., Vennapusa, P., Tutumluer, E., Vavrik, W., Moaveni, M., Gillen, S. (2018). "Spatial verification of modulus for pavement foundation system." *Transportation Research Record*, Journal of the Transportation Research Board (in print).

<https://doi.org/10.1177/0361198118782266>

White, D. J., and Vennapusa, P. (2017). "2017 MnROAD Unbound Layer Evaluation Using Intelligent Compaction: Ingios Validated Intelligent Compaction (VIC) Results." Final Report No. 2017-043, Ingios Geotechnics.

[http://www.dot.state.mn.us/mnroad/nrra/structureandteams/geotechnical/documents/FINAL\\_Ingios%20VIC%20Compaction%20Report\\_MnROAD\\_v7.pdf](http://www.dot.state.mn.us/mnroad/nrra/structureandteams/geotechnical/documents/FINAL_Ingios%20VIC%20Compaction%20Report_MnROAD_v7.pdf)